

X-ray diffraction of ordered mesoporous materials: High precision at small-angle regions

1. Background

The metal oxide catalyst support is the backbone of heterogeneous catalysis and has been studied extensively for decades.⁽¹⁾ Traditionally, the support itself is not catalytically active; instead, the support increases the stability and specific surface area of the catalyst. Currently, the most studied supports include SiO₂, Al₂O₃, TiO₂, and carbon-based materials.⁽²⁻⁵⁾ Among these, SiO₂ has many practical advantages including availability of raw materials, low cost, and chemical stability.

Among many different structures of SiO₂, large-pore zeolites are in demand for separation processes involving macromolecules. The SiO₂-based zeolite synthesis method is simple, customizable, and results in materials with good structural stability. Since the discovery of the hexagonally ordered MCM-41 mesoporous zeolite by Beck et al.,⁽⁶⁾ surfactant template synthesis technology has expanded to a variety of material systems. These materials are usually prepared under the condition of simultaneous silica-surfactant self-assembly and inorganic condensation, resulting in meso-ordered composites. The synthesis of MCM-41 materials requires the use of ionic surfactants as guides, most commonly cetyltrimethyl bromide (CTAB). MCM-41 has a hexagonal structure (P6mm space group), and the pores form a one-dimensional ordered structure with pore diameters ranging from 2-7 nm, shown in Figure 1a.

Following the synthesis of MCM-41, a series of ordered mesoporous silicate materials were synthesized by Zhao et al. using triblock polymers as template agents, including SBA-15.⁽⁷⁾ SBA-15 has a hexagonal structure similar to MCM-41 (P6mm space group), but with larger mesopore sizes (5-15 nm), thicker pore walls (3.1-6.4 nm), high thermal and hydrothermal stability, and interconnected micropores, shown in Figure 1b.⁽⁸⁾ SBA-15 holds great potential in the field of catalysis, and its unique

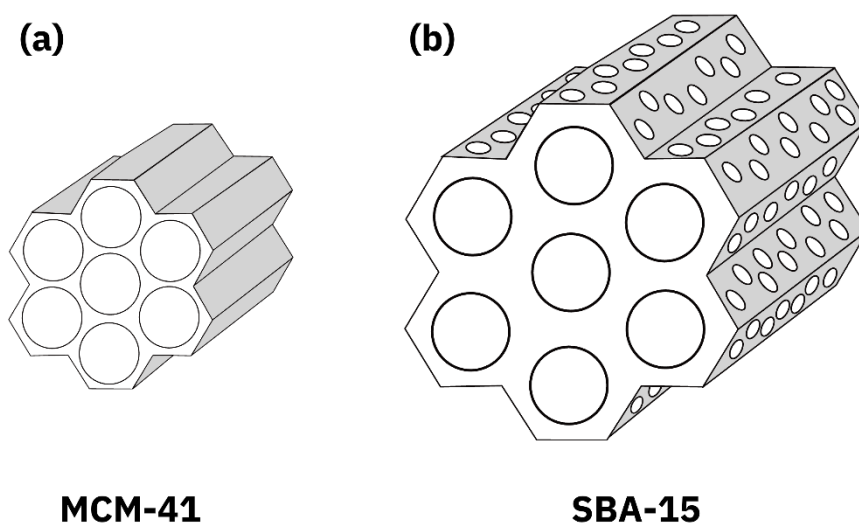


Figure 1: Illustration comparing the structures of MCM-41 (a) and SBA-15 (b), not to scale

combination of micro and mesopores play a key role in the adsorption of reactive molecules.

The crystal structures of ordered materials are often studied using X-ray diffraction (XRD). X-rays with a specific wavelength are irradiated onto a crystal at various incident angles, and diffraction is observed at specific angles when Bragg's law is satisfied (Eqn. 1). The structure is characterized by recording the diffraction angles and the intensities of the corresponding diffraction peaks. Due to the large pore spacing of SBA-15, diffraction occurs at very low angles (typically $< 5^\circ$), at which peak intensities are typically weak and difficult to resolve. Additional techniques like small-angle X-ray scattering (SAXS) have been developed for this purpose, but these require specialized instrumentation. Small-angle XRD patterns can still be obtained using a powerful and accurate X-ray diffractometer equipped with a vertical theta/theta goniometer.

$$\text{Bragg's Law: } n\lambda = 2d \sin \theta \quad (1)$$

Where:

n = order of reflection (integer)

λ = wavelength of incident X-rays

d = interplanar spacing of crystal

θ = angle of incidence

In combination with XRD, the pore structure can be determined by gas adsorption methods using various subcritical fluid molecular probes (N_2 , Ar, and CO_2). N_2 adsorption at 77 K is often used to characterize the specific surface area, total pore volume and pore size distribution of mesoporous materials.

2. Experiment

In this application note, two SBA-15 samples were prepared at different crystallization temperatures. SBA-15 Sample 1 was crystallized at 100 °C for 24 hours, and SBA-15 Sample 2 was crystallized at 120 °C for 24 hours. The phase composition of SBA-15 samples under different synthesis conditions was characterized by an **AMI Lattice PRO X-ray diffractometer** (Cu target, $\lambda=0.1548\text{nm}$) from $2\theta = 0.5$ to 4° . Secondly, the **AMI Matrix 1000** physical adsorption instrument was used to analyze the specific surface area, pore size and pore volume of the samples.

3. Results

X-ray diffraction can effectively analyze the structural characteristics of mesoporous materials in space groups. Figure 2 shows the XRD spectra of both SBA-15 samples which have similar characteristic peaks, and three clearly visible characteristic peaks appear at 0.93° , 1.603° , and 1.821° , which correspond to the crystal plane diffraction of (100), (110) and (200) symmetry of the P6mm space group of the hexagonal crystal system. According to the Bragg equation (Eq. 1), the strong (100) crystal plane diffraction peak can calculate the corresponding crystal plane spacing; More importantly, according to the structure-activity relationship between the unit cell parameters and the crystal plane spacing of the crystal geometry hexagonal crystal system ($a=2d/\sqrt{3}$), the unit cell parameter a value of SBA-15 can be calculated, shown in Table 1.

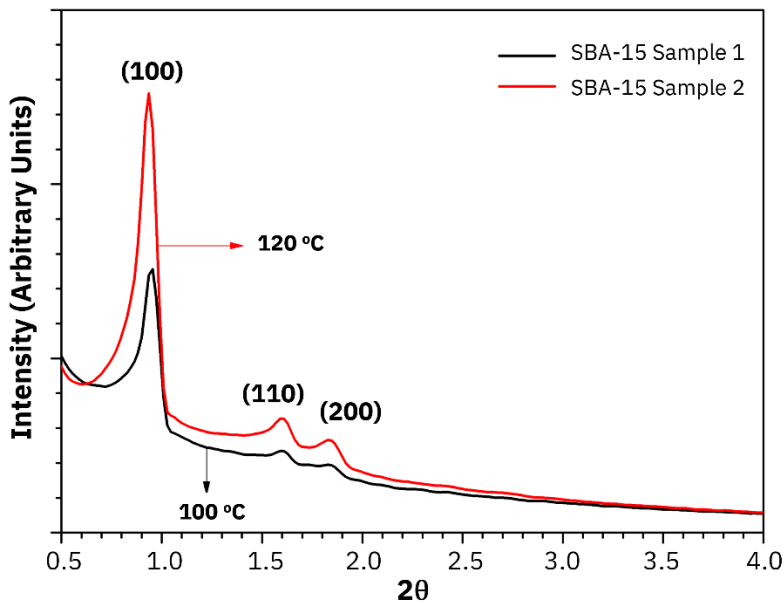


Figure 2: XRD spectra of SBA-15 zeolites crystallized at 100 °C (black curve) and 120 °C (red curve)

All three diffraction peak intensities increased with increased crystallization temperature. When the crystallization temperature was low, the hydrophobic swelling agent (polypropylene oxide) was less likely to form micelles, the crystallization was reduced, and the diffraction peaks of the (110) and (200) crystal surfaces were weaker (Fig. 2, black curve). The increase of diffraction peak intensity with temperature indicates improved silicate polymerization. Additionally, the hydrophilicity of the template agent (polyethylene oxide) was weakened, which promoted micelle formation, and resulted in improved pore

ordering of the zeolite. Secondly, when the crystallization temperature increased, the diffraction angles of the three peaks were offset to a smaller angle, indicating that the unit cell parameter a of the material increased. This correlated well with the increased pore size.

| Crystallization temperature (°C) | d(100) (Å) | Unit cell parameter a (Å) | BET specific surface area (m ² /g) | Pore size (Å) | Pore volume (cm ³ /g) | Wall thickness (Å) |
|----------------------------------|------------|---------------------------|---|---------------|----------------------------------|--------------------|
| 100 | 92.87 | 107.24 | 717.086 | 60.263 | 0.966 | 46.97 |
| 120 | 94.54 | 109.17 | 852.896 | 63.695 | 1.169 | 45.48 |

Table 1: XRD and N₂ adsorption-desorption isotherm results for SBA-15 samples

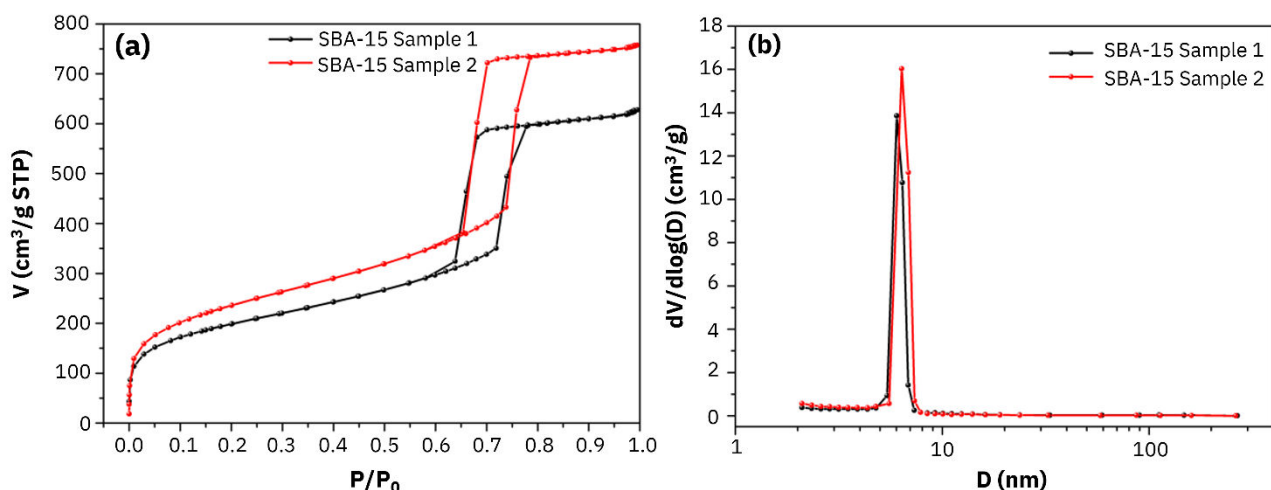


Figure 3: a) N₂ adsorption-desorption isotherms and b) pore size distributions of SBA-15 zeolites crystallized at 100 °C (black curve) and 120 °C (red curve)

The N₂ adsorption-desorption isotherms are shown in Figure 3a. Both SBA-15 samples exhibited Type IV isotherms with H1 type hysteresis loops, which are indicative of mesoporous ordered materials with uniform pore size distribution. Additionally, the relative pressure of capillary condensation ($P/P_0 = 0.6 - 0.8$) increased slightly with increased temperature, indicating that the pore size increased. This pore size effect was confirmed in the pore size distribution curve, shown in Figure 3b. For mesoporous zeolites in the P6mm space group, the pore wall thickness can be calculated by the difference between the unit cell parameter a and the pore size, and the results are shown in Table 1. Larger pores formed in SBA-15 Sample 2 resulted in decreased wall thickness.

4. Conclusions

The SBA-15 materials synthesized with different crystallization temperatures were examined by XRD and N₂ adsorption-desorption isothermal characterization. The corresponding crystal plane spacing and the unit cell parameter a value of SBA-15 was calculated according to crystal geometry. The specific surface area and pore volume of the material were analyzed by isothermal N₂ physical adsorption, showing a mesoporous material with capillary condensation. With these detailed characterization techniques, it was observed that the specific surface area, pore volume, and pore diameter increased with the increase of crystallization temperature.

These sensitive, small-angle diffraction measurements were possible using the powerful **LatticePRO XRD** from AMI, shown in Figure 4. The **Lattice Series** offers customizable instruments with optional upgrades that improve functionality and data sensitivity. The theta-theta goniometer included with the **LatticePro XRD** minimizes sample displacement and height errors, which distort peaks at low angles. Additionally, the 1600 W X-ray source improves signal to noise ratios at low diffraction angles. These features allow for reliable low-angle measurements in an affordable, benchtop configuration.

The **Matrix 1000**, shown in Figure 4, is also a powerful and customizable gas sorption analyzer platform designed for complex systems, allowing for both micropore and mesopore analysis.

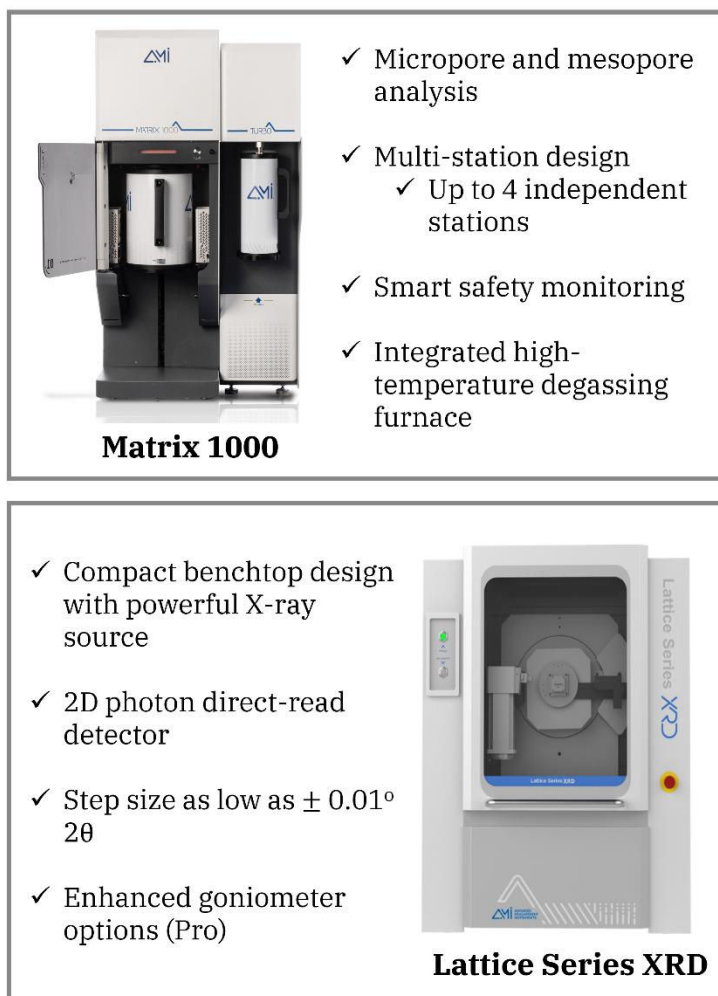


Figure 4: Highlighted features of Matrix 1000 (top) and Lattice Series XRD (bottom) from AMI

5. References

- (1) Boudart, M. Catalysis by supported metals. *Adv. Catal.* **1969**, *20*, 153-166.
- (2) Min, B. K.I; Santra, A. K.; Goodman, D. W. Understanding silica-supported metal catalysts: Pd/silica as a case study. *Catal. Today*, **2003**, *85*, 113-124.
- (3) Trueba, M. and Trasatti, S. P. γ -Alumina as a support for catalysis: A review of fundamental aspects. *Eur. J. Inorg. Chem.* **2005**, *2005*, 3393-3403.
- (4) Sebastian, J.; Mebrahtu, C.; Zeng, F.; Palkovits, R. Strong metal-support interaction on TiO₂-supported metal catalysts for fine-tuning catalysis. *Angew. Chem., Int. Ed.* **2026**, *65*, e02611.
- (5) Rodríguez-Reinoso, F.; Sepúlveda-Escribano, A. Carbon as catalyst support. *Carbon materials for catalysis*; Serp, P.; Figueiredo, J. L., Eds.; John Wiley & Sons, 2009; pp 131-155.
- (6) Beck, J. S.; Vartuli, Roth, W. J.; Leonowicz, M. E.; Kresge, C. T.; Schmitt, K. D.; Chu, C. T-W.; Olson, D. H.; Sheppard, E. W.; McCullen, S. B.; Higgins, J. B.; Schlenker, J. L. A new family of mesoporous molecular sieves prepared with liquid crystal templates. *J. Am. Chem. Soc.* **1992**, *114*, 10834-10843.
- (7) Zhao, D.; Feng, J.; Huo, Q.; Melosh, N.; Fredrickson, G. H.; Chmelka, B. F.; Stucky, G. D. Triblock copolymer syntheses of mesoporous silica with periodic 50 to 300 angstrom pores. *Science*, **1998**, *279*, 548-552.
- (8) Ryoo, R.; Ko, C. H.; Kruk, M.; Antochshuk, V.; Jaroniec, M. Block-copolymer-templated ordered mesoporous silica: Array of uniform mesopores or mesopore-micropore network? *J. Phys. Chem. B*, **2000**, *104*, 11465-11471.